

# T-Slot Design for an Enhanced Electromagnetic Band Gap to Reduce Mutual Coupling in MIMO Antennas

Nopphadon Phusam<sup>1</sup>, Artitiphong Sangthong<sup>1\*</sup>, Thanakarn Suangun<sup>1\*</sup>,

Nutyada Nantapanich<sup>2</sup>, and Buntueng Yana<sup>1</sup>

<sup>1</sup>Department of Electrical Engineering, Faculty of Engineering, University of Phayao, Thailand, ph.nopphadon@gmail.com,s.artitiphong@gmail.com\*,thanakarn.su@up.ac.th\*,mr.buntueng@gmail.com, 

<sup>2</sup>Department of Thai-German Pre-Engineering School, Faculty of The College of Industrial Technology, King Mongkut's University of Technology North Bangkok, Bangsue, Bangkok, Thailand, nutyadan@kmutnb.ac.th

#### Abstract

The paper presents an enhanced Electromagnetic Band Gap (EBG) structure designed to significantly reduce mutual interaction among closely spaced antenna components. This enhancement is accomplished by the incorporation of a wave isolation mechanism consisting of two rectangular elements incorporated into the EBG design. These coatings function as both electromagnetic and physical barriers. The T-slot EBG design has a 2×8 periodic unit cell array tuned for peak efficiency at a frequency of 2.45 GHz. This architecture is often used in wireless communication systems adhering to the IEEE 802.11b/g/n specifications. The isolation efficacy of the suggested T-slot EBG design is markedly enhanced, as shown by experimental and simulation findings. This yields a decrease in mutual coupling of 15 dB compared to traditional systems. The antenna radiation pattern is maintained, and the rear lobe radiation is significantly decreased, with a 10 degree shift towards the XY plane. In the frequency range of 2.39 to 2.96 GHz, the T-slot EBG system has a bandgap of 21.31%. The results confirm that the T-slot EBG design is a suitable option for high-performance wireless and MIMO applications, since it enhances antenna array performance by reducing undesirable electromagnetic interactions.

**Keywords:** Electromagnetic band gap (EBG), T-slot design, multiple-input multiple-output (MIMO), isolation, radiation pattern.

# 1. Introduction

At present, the requirement for sustainable high-speed wireless communication systems, including Industrial Internet of Things (IIoT) devices and Wi-Fi networks, has propelled the widespread use of multiple-input-multiple-output (MIMO) technology [1,2]. MIMO systems enhance data throughput by employing multiple antennas at both the transmitter and receiver, thereby supporting a greater number of users. However, mutual coupling between closely spaced antenna elements significantly degrades performance. In typical MIMO antenna arrays with closely spaced elements, the envelope correlation coefficient (ECC) often rises beyond acceptable levels, resulting in degraded isolation and reduced channel capacity.

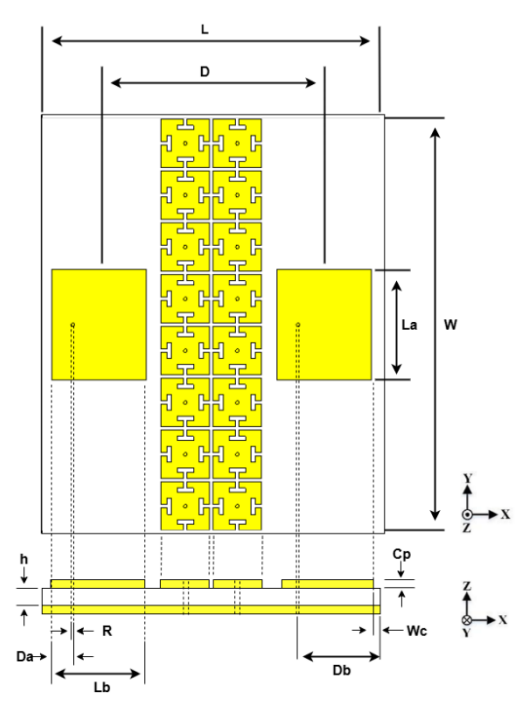


Figure 1. The Dimensions of the proposed antennas with the T-Slot  $\operatorname{EBG}$ 

Furthermore, the radiation pattern can become distorted, and the resonance frequency can shift due to unwanted interactions with nearby conductive materials when electronic components or conductors are situated close to the antenna structures. These challenges can lead to an increase in the envelope correlation coefficient (ECC) and a reduction in channel capacity [3].

Previous studies have explored various methods for reducing mutual coupling in MIMO systems. For example, defected ground structures (DGS) are highly effective for enhancing signal separation at 22 dB of the workpiece, despite the fact that their design complexity remains a challenge. Despite their outstanding performance at lower frequencies, metamaterial-inspired antennas suffer deterioration in higher frequency bands [4]. Complementary split-ring resonators (CSRRs) significantly enhance isolation, achieving 22.4 dB and 31.5 dB for the unstructured and fluted configurations, respectively. The efficient isolation of multi-port systems is enhanced by the greater degree of isolation. This

<sup>\*</sup>Corresponding Author

วันที่ 19-21 พฤศจิกายน 2568 ณ โรงแรมฟราม่า จังหวัดเชียงใหม่

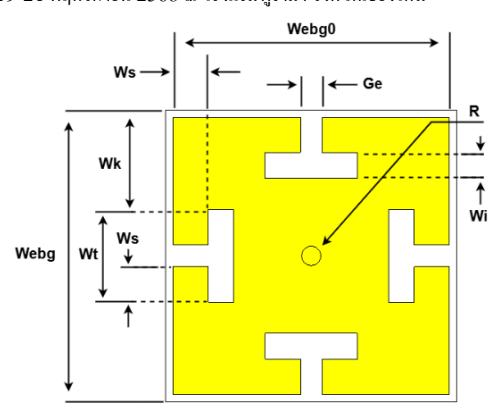


Figure 2. Geometry of the T-slot EBG unit cell

enhancement, however, presents physical design challenges that may compromise directional stability and positioning accuracy, resulting in variations in radiation patterns of 60 degrees and 25 degrees. [5, 6]. Parallelcoupled resonators (PCRs) have remarkable multi-band capabilities and omnidirectional transmission; however, they utilize resistors for modulation and directional regulation. Moreover, there exists a potential for interference at concurrently functioning frequencies. [7] Meanwhile, frequency-selective surfaces (FSSs) use slotbased techniques to control emitted or reflected frequencies. The transmission isolation level is -30 dB, covering the bandwidth of 23.63-32.90 GHz, and offers a tilt angle of 15 degrees. The main limitation of FSS in this approach is that its efficacy is contingent upon the angle at which the electromagnetic wave strikes the item, rendering it troublesome for mobile systems or settings with variable angles. Consequently, FSSs are mostly confined to high-frequency configurations. [8].

The aforementioned approaches can be broadly classified under electromagnetic wave control techniques, which have been extensively investigated to address the stated limitations. This category aims to improve antenna performance through modifications in material characteristics and structural configurations. Among these, electromagnetic band gap (EBG) structures represent a particularly effective solution [9-11]. The primary objective of EBGs is to enhance isolation by suppressing surface waves while minimally affecting the desired wave propagation. Typically, EBGs employ periodic arrangements of unit cells, which can be tailored to generate bandgaps at specific target frequencies by appropriately modifying their geometrical features, such as the positioning of T-shaped slots.

This work presents an innovative EBG-T slot configuration to address the connectivity challenges of 2.45 GHz MIMO systems (IEEE 802.11b/g/n). The suggested technique attempts to achieve two key objectives: first, to substantially decrease mutual coupling while preserving system bandwidth, and second, to reduce distortion in the radiation pattern. The suggested wireless system is ultimately informed by practical insights derived from the systematic advancement of the project,



including the intricate design of the antenna and T-slot EBG, followed by analytical dispersion analysis and experimental validation.

# 2. Antenna Design

The proposed design, intended for operation at 2.45 GHz, consists of two symmetrical microstrip rectangular patch antennas. L × W = 102.9 mm × 123.5 mm are the board's overall dimensions. The antenna is fabricated on a FR-4 substrate with a thickness (h) of 1.6 mm, a copper thickness (cp) of 0.035 mm, a relative permittivity ( $\varepsilon_r$ ) of 4.3, and a loss tangent (tan  $\delta$ ) of 0.019, as illustrated in Figure 1. Equation (1) employs these material parameters to calculate the effective dielectric constant ( $\varepsilon_{eff}$ ), which is then used in Equation (2) to determine the guided wavelength ( $\lambda_g$ ).

$$\varepsilon_{eff} = \left(\frac{\varepsilon_r + 1}{2}\right) + \left(\frac{\varepsilon_r - 1}{2}\right) \left(1 + 12\frac{h}{W}\right)^{-1/2} \tag{1}$$

$$\lambda_{\rm g} = \frac{\lambda_0}{\sqrt{\epsilon_{eff}}} \tag{2}$$

The wavelength of the two rectangular patch antennas is about half that of the guide wavelength. The resonance frequency of 2.45 GHz may be altered by adjusting the patch dimensions to La = 33 mm and Lb = 28 mm. This configuration is equivalent to a side-by-side at the E Plane design with a distance of D = 66.9 mm. The two antennas were connected via a 50  $\Omega$  SMA probe with a fed diameter (d) of 1 mm. The connections are positioned at the fed location on the rectangle, with dimensions Da = 6.4 mm and Db = 25.7 mm. The width between the left and right borders of Reduction of Surface Wave Reflections or Edge Effects in Antenna Substrates [12] is Wc = 4 mm.

In the next step, a T-slot EBG is placed between the two antennas to reduce mutual coupling, as seen in Figure 2. Each unit cell measures about 0.125λω to provide optimum suppression of surface waves around the operating frequency [13]. The wave gap develops from the inductive-capacitive (LC) characteristics of the unit cell, which significantly restricts the frequency range in which electromagnetic waves may travel. Equation (3) of the unit cell illustrates how the resonance frequency of 2.45 GHz may be calculated utilizing a similar circuit model.

$$f_0 = \frac{1}{2\pi\sqrt{LC}} \tag{3}$$

The EBG specifies an inductance (L) of 0.91 nH and a capacitance (C) of 5.62 pF, determined by the unit cell's physical dimensions, including gap spacing, conductor width, and the dielectric characteristics of the supporting material. The T-slot unit cell was specifically designed to get the requisite gap wave characteristics for this study. The implemented geometrical parameters are Webg = 15.4 mm, Webg0 = 14.4 mm, We = 1.8 mm, Wk = 3.2 mm, Wt = 4.8 mm, and Ge = 1.1 mm, with the via hole

วันที่ 19-21 พฤศจิกายน 2568 ณ โรงแรมฟราม่า จังหวัดเชียงใหม่

diameter set to r=1 mm. The exact setting of these parameters to create a band gap in the 2.45 GHz geography efficiently reduces surface current propagation and enhances mutual signal separation between adjacent MIMO antennas.

The electromagnetic bandgap (EBG) properties of the proposed design will be validated by the dispersion diagram shown in Figure 3, which illustrates the connection between frequency and wave number (k). indicates the spatial periodicity and phase modulation of electromagnetic waves propagating via the periodic EBG structure. The parameter k may be understood as the rate of phase variation and the direction of wave propagation as it moves across the periodic unit cells of the EBG lattice. The dispersion diagram is assessed along the highsymmetry direction  $\Gamma \rightarrow X \rightarrow M \rightarrow \Gamma$ , using the x-axis inside the primary Brillouin zone [13]. This approach illustrates the anisotropic characteristics of the structure by including important directions of wave propagation. The point  $\Gamma$  represents the center of the Brillouin zone (k = 0), whilst X and M signify symmetry points situated at the borders and corners of the zone, respectively. The dispersion characteristics along this path are analyzed in order to provide a comprehensive evaluation of wave propagation within the EBG structure and, more importantly, to identify bandgap frequencies, which are regions where electromagnetic wave propagation is prohibited.

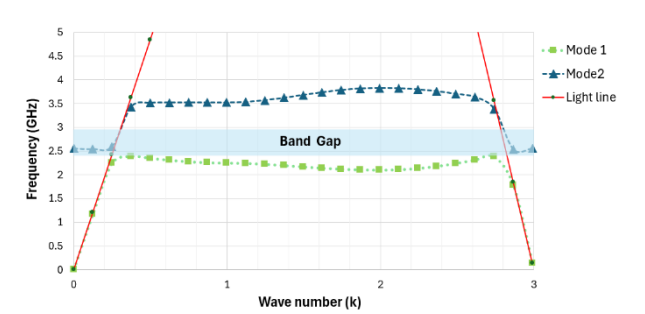


Figure 3. Dispersion diagram of the proposed T-slot EBG

The dispersion diagram delineates two characteristic eigenmodes: Mode 1 Transverse Magnetic (TM) and Mode 2 Transverse Electric (TE). In mode 1, a longitudinal electric component exists, but in mode 2, the electric field is totally transverse to the direction of propagation. Identifying these modes is important for analyzing the impact of the EBG structure on bandgap development and wave propagation. The light line, indicating wave propagation in open space, serves as a reference. Modes located below the light line are often confined inside the structure, whilst those above it possess the capacity to radiate. This observation supports the EBG's capacity to contain energy and prevent the propagation of harmful waves. The presence of a frequency range without propagating modes indicates the existence of an electromagnetic bandgap. This claim is further confirmed by the finding of phase changes at symmetry locations and the absence of mode curves. The



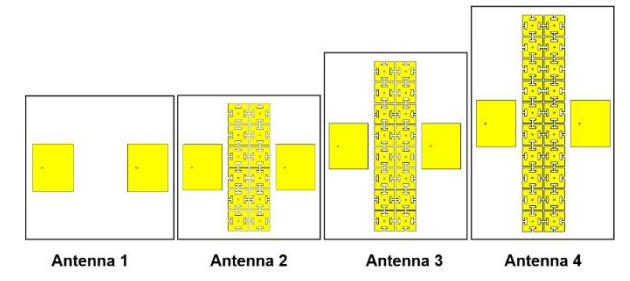


Figure 4 The Evolution of Design and the implementation of EBG for the analysis of the proposed unit cell.

bandgap of 2.39 to 2.96 GHz, representing a 21.31% fractional bandwidth, signifies an extensive reduction of wave transmission. This stopband illustrates the efficacy of the EBG structure in reducing mutual coupling and surface wave interference in MIMO systems operating at 2.45 GHz.

# 3. Experimental and Result

The CST Studio Suite program will be used to analyze the impact of the EBG structure on the performance of the MIMO antenna, with the antenna's location remaining constant. The objective is to use the EBG, which is designed to form a barrier. Antenna 1, simulated with three more antenna designs, represents the baseline devoid of an EBG structure. EBG walls with 2 × 6,  $2 \times 8$ , and  $2 \times 10$  unit cells are integrated into antennas 2, 3, and 4, respectively (Figure 4). As the number of EBG cells increases, the S-parameter test results (Figure 5) indicate enhancements in impedance matching  $(S_{11})$  and a reduction in coupling  $(S_{21})$ . The  $S_{11}$  values for all antennas are around -17 dB; however, the S<sub>21</sub> values for Antennas 3 and 1 vary by up to 15 dB at 2.45 GHz. The  $S_{\rm 21}$ measurements of Antennas 3 and 2 show a discrepancy of about 4 dB The experimental findings indicate that antennas 3 and 4 function at optimal efficiency, exhibiting an average S<sub>21</sub> value of -37 dB Antenna 4 has a somewhat higher separation, about 1 dB inferior to antenna 3; however, it also covers a wider physical region. It also includes a broader geographic region. Antenna 3, with 2 × 8 unit cells, is considered the most optimal configuration because of its outstanding performance and compact construction, therefore avoiding excessive size

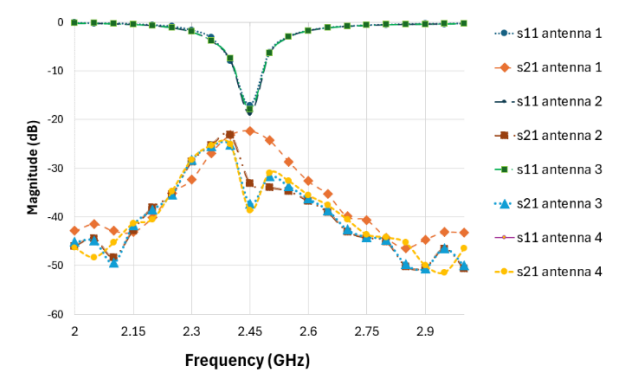


Figure 5 The Simulated results of the EBG design Evolution are shown through the reflection coefficients (S11) and transmission coefficients (S21).

วันที่ 19-21 พฤศจิกายน 2568 ณ โรงแรมฟราม่า จังหวัดเชียงใหม่

enhancement. This confirms that the adoption of EBG in MIMO systems is important for wireless applications, since antenna 3 has superior impedance and signal separation characteristics compared to antenna 1

To determine the efficacy of MIMO antennas with differing antenna splits, supplementary experiments are conducted. Following the determination that the 2×8 EBG unit cell structure attains an optimal equilibrium between efficiency and dimensions at 2.45 GHz,

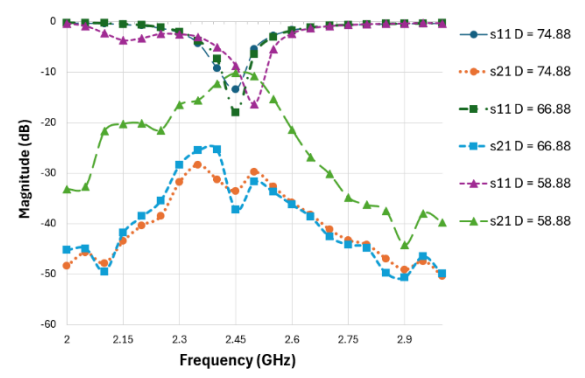


Figure 6 The simulated results of the EBG design with adjusted antenna spacing are presented using the reflection coefficients  $(S_{11})$  and transmission coefficients  $(S_{21})$ .

The EBGs are positioned at different distances (D) from the antenna, as seen in Figure 6. The S<sub>11</sub> value of about -8 dB and the S21 value of -10 dB indicate that a distance of 0.48\(\lambda\), equivalent to 58.88 mm, from the EBG to the closest point is inadequate for effective impedance matching. This indicates that the spacing is inadequate for correctly separating the antenna components, leading to distorted S<sub>11</sub> values at other frequencies of -13 dB and altered radiation patterns. This ultimately results in an enhancement of S<sub>21</sub> values. The experimental mid-range distance is 0.58λ<sub>0</sub>, equivalent to 66.88 mm, with S<sub>11</sub> values of -17 dB and  $S_{21}$  values of -37 dB. The distance of  $0.62\lambda_0$ , measuring 74.88 mm, is the greater distance, with S<sub>11</sub> and S<sub>21</sub> values recorded at -33 dB. The measured distance of 66.88 mm is the ideal distance for applications demanding good impedance matching and great isolation between the antenna, as shown by the experimental results.

Figure 7 illustrates the fabrication of a physical prototype of a MIMO antenna system to rigorously confirm the simulation findings and assess the practical performance of the developed system. This prototype has an antenna distance of 66.88 mm and an improved 2 × 8 EBG unit cell configuration. The prototype was fabricated on an economical FR-4 substrate with the conventional PCB etching method. Subsequently, the S parameters were precisely measured in a controlled setting and calibrated using a FieldFox-N9923A. Results were then contrasted with the appropriate simulation results shown in Figure 8. The modeling and discovered results indicate virtually identical trends in S<sub>11</sub> and S21; however, slight variations exist. The resonant frequency of the observed S<sub>11</sub> presents a little deviation of roughly 2.45 GHz relative to the predicted S<sub>11</sub>. This deviation may stem from multiple factors, including manufacturing inconsistencies



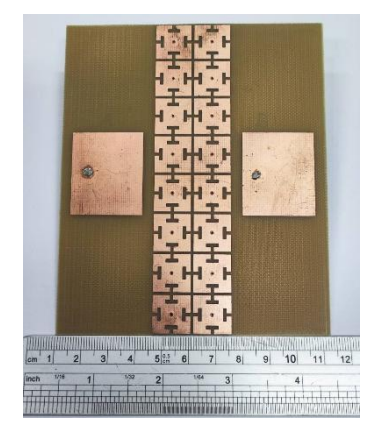


Figure 7 Prototype of the Proposed MIMO Antenna System with EBG Structure

in the PCB etching process, minor variations in the electrical properties of the actual FR-4 material utilized in the prototype compared to the simulation values, connector losses, possible solder defects, and background noise or fundamental inaccuracies in the measurement apparatus. The rectangular patch antenna coupled with the T-slot EBG design provides maximum gains of 10 degrees and 350 degrees for the left and right antennas, respectively, in the XZ-plane (A), as depicted in Figure 9. Moreover, it exhibits a lower rear lobe relative to a traditional antenna. Furthermore, both antennas have a maximum gain of 0 degrees in the YZ plane (B). The EBG structure influences the overall radiation properties, producing a unidirectional radiation pattern. The experimental findings verify the simulation-driven design technique, illustrating the practical viability of incorporating a compact EBG wall into a MIMO antenna system operating in the 2.4 GHz ISM band to improve performance.

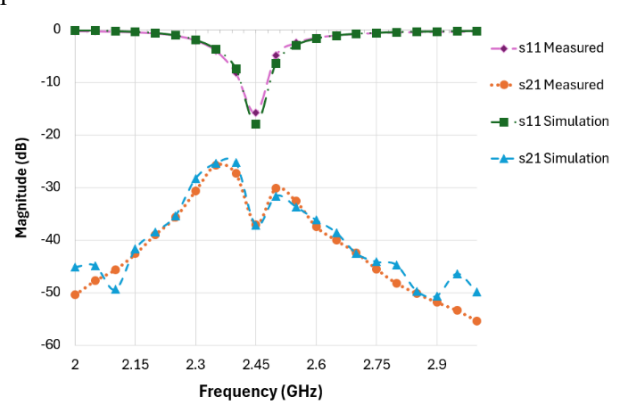


Figure 8 Simulated and Measured results of the proposed antenna with the T-Slot EBG, showing the reflection coefficients  $(S_{11})$  and transmission coefficients  $(S_{21})$ .

# 4. Conclusion

This work presents a compact T-slot EBG structure that improves MIMO antenna isolation by 14.9 dB in the 2.39–2.96 GHz band by suppressing surface waves and minimizing coupling. The design achieves size efficiency and operates within the 2.45 GHz ISM band (IEEE

วันที่ 19-21 พฤศจิกายน 2568 ณ โรงแรมฟราม่า จังหวัดเชียงใหม่

802.11b/g/n), making it suitable for IoT, Wi-Fi, and industrial systems. Potential applications also include wireless sensor networks, wearable devices, vehicular communications, and UAV platforms. Future research may explore reconfigurable designs and multi-band scalability for 5G/6G integration.

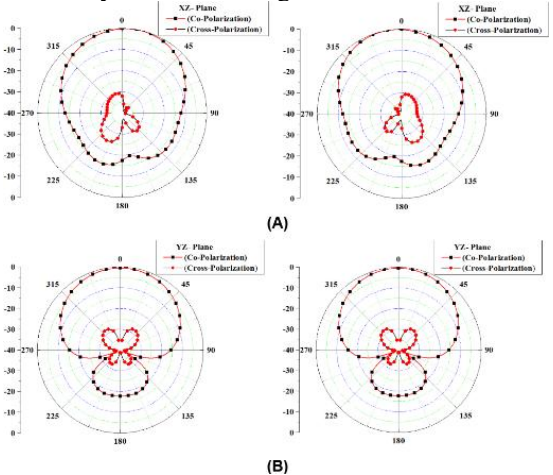


Figure 9 Radiation patterns of the proposed antenna with the EBG T-Slot Design at the resonance frequency of 2.45 GHz. (A) XZ-plane and (B) YZ- plane.

# 5. Acknowledgments

This thesis research was supported by a grant from the University of Phayao.

#### References

- [1] Wang, H., et al., Isolation Improvement and Bandwidth Enhancement of Dual-Band MIMO Antenna Based on Metamaterial Wall. IEEE Antennas and Wireless Propagation Letters, 2025. 24(5): p. 1144-1148.
- [2] Chutchavong V.,et al., A Flexible and Compact UWB MIMO Antenna with Dual-Band-Notched Double U-Shaped Slot on Mylar® Polyester Film. Electronics, 2025. 14: p. 1-24.
- [3] Khan, A., et al., Mutual Coupling Reduction Using Ground Stub and EBG in a Compact Wideband MIMO-Antenna. IEEE Access, 2021. 9: p. 40972-40979.
- [4] Megahed, A.A., et al., Sub-6 GHz Highly Isolated Wideband MIMO Antenna Arrays. IEEE Access, 2022. 10: p. 19875-19889.
- [5] Wang, P., et al., Wideband Gain Enhancement of High-Isolation and Quasi-Omnidirectional Metamaterial MIMO Antenna for Vehicular Radar. IEEE Transactions on Instrumentation and Measurement, 2022. 71: p. 1-12.
- [6] H., T., and B. Roy, Low-Profile CO-CSRR and EBG Loaded Tri-Quarter Circular Patch EWB MIMO Antenna With Multiple Notch Bands. IEEE Open Journal of Antennas and Propagation, 2024. 5(3): p. 634-643.
- [7] Park, J.D., M. Rahman, and H.N. Chen, *Isolation Enhancement of Wide-Band MIMO Array Antennas*



- *Utilizing Resistive Loading.* IEEE Access, 2019. 7: p. 81020-81026.
- [8] Ahmad, J., and M. Hashmi, Reduced Inter-Element Interference mmWave MIMO Antenna and Its Application in WBAN. IEEE Access, 2025. 13: p. 70947-70963.
- [9] Althuwayb, A.A., et al., Metasurface-Inspired Flexible Wearable MIMO Antenna Array for Wireless Body Area Network Applications and Biomedical Telemetry Devices. IEEE Access, 2023. 11: p. 1039-1056.
- [10] Wongsin, N., et al. *Improvement of Isolation with EBG Wall Applied by E Model Structure for IEEE 802.11b/g/n.* in 2021 9th International Electrical Engineering Congress (iEECON). 2021.
- [11]Li, W., et al., Bandwidth Enhancement and Isolation Improvement in Compact UWB-MIMO Antenna Assisted by Characteristic Mode Analysis. IEEE Access, 2024. 12: p. 17152-17163.
- [12] Balanis, C.A., *Antenna Theory: Analysis and Design*, in *Modern Antenna Handbook*. 2016, Wiley: Hoboken, NJ, USA. p. 819.
- [13] Ahmed, A., M.R. Robel, and W.S.T. Rowe, *Dual-Band Two-Sided Beam Generation Utilizing an EBG-Based Periodically Modulated Metasurface*. IEEE Transactions on Antennas and Propagation, 2020. 68(4): p. 3307-3312.



Nopphadon Phusam received the Bachelor's Degree in Electrical Engineering from the University of Phayao (UP), Phayao, Thailand, in 2018. He is currently pursuing the master's degree in electrical engineering with the Department of Electrical Engineering, Faculty of Engineering, University of Phayao. His research interests include metamaterials, MIMO antennas, and deep learning.



**Artitiphong Sangthong** graduated from Thatako Pittayakhom School in 2021. I am currently studying for a bachelor's degree in the Faculty of Engineering, Department of Electrical Engineering, University of Phayao. Current research interests: metamaterials in antennas.



Thanakarn Suangun received B.Eng., M.Sc. in Communication Engineering, and Ph.D. degrees in Electrical Engineering from King Mongkut's University of Technology North Bangkok (KMUTNB), Thailand, in 2006, 2009, and 2020, respectively. Since 2012, he has been a lecturer at the Department of Electrical Engineering, School of Engineering, University of Phayao, Thailand. His research interests include RF/microwave, multiband small antennas for communication applications, and automation.

### การประชุมวิชาการทางวิศวกรรมไฟฟ้า ครั้งที่ 48

The 48<sup>th</sup> Electrical Engineering Conference (EECON-48)

วันที่ 19-21 พฤศจิกายน 2568 ณ โรงแรมฟูราม่า จังหวัดเชียงใหม่



Nutyada Nantapanich received her B.Eng. in Chemical Engineering from King Mongkut's University of Technology North Bangkok in 2006 and M.Eng. in Chemical and Environmental Engineering from Burapha University, in 2014. Her master's independent study focused on wastewater treatment from tank-cleaning processes using

electrocoagulation with both monopolar and bipolar electrodes. She is currently pursuing a Ph.D. in Electrical Engineering at Rajamangala University of Technology Thanyaburi, where her research is centered on chemical detection sensors.



Buntueng Yana (Member, IEEE) received B.Eng. and M.Eng. degrees in Electrical Engineering from Chiang Mai University, Thailand, in 2006 and 2009, respectively, and a Ph.D. in Information Science and Technology from Osaka University, Japan, in 2019. He is currently a lecturer with the Department of Electrical Engineering at the University of Phayao, Thailand, where he began his academic career. His research interests include robotics, automatic control, power generation, and the application of machine learning to medical applications

